Nature of phase transitions in a generalized complex $|\psi|^4$ model

Elmar Bittner and Wolfhard Janke
Institut für Theoretische Physik, Universität Leipzig, Augustusplatz 10/11, D-04109 Leipzig, Germany
(Received 30 July 2004; published 21 January 2005)

We employ Monte Carlo simulations to study a generalized three-dimensional complex $|\psi|^4$ theory of Ginzburg-Landau form and compare our numerical results with a recent quasianalytical mean-field-type approximation, which predicts first-order phase transitions in parts of the phase diagram. As we have shown earlier, this approximation does not apply to the standard formulation of the model. This motivated us to introduce a generalized Hamiltonian with an additional fugacity term controlling implicitly the vortex density. With this modification we find that the complex $|\psi|^4$ theory can, in fact, be tuned to undergo strong first-order phase transitions. The standard model is confirmed to exhibit continuous transitions which can be characterized by *XY* model exponents, as expected by universality arguments. A few remarks on the two-dimensional case are also made.

DOI: 10.1103/PhysRevB.71.024512 PACS number(s): 74.20.De, 02.70.Uu, 64.60.−i

I. INTRODUCTION

For a long time the Ginzburg-Landau model has been considered as paradigm for studying critical phenomena using field-theoretic techniques.[1] Perturbative calculations of critical exponents and amplitude ratios of the Ising ($n=1$), *XY* ($n=2$), Heisenberg ($n=3$), and other $O(n)$ spin models relied heavily on this field-theoretic formulation.[2] Even though the spin models contain only directional fluctuations, while for n-component Ginzburg-Landau fields with $n \geqslant 2$ directional and size fluctuations seem to be equally important, the two descriptions are completely equivalent, as is expected through the concept of universality and has been proved explicitly for superfluids with $n=2$, where the spin model reduces to an *XY* model.[3] Therefore it appeared as a surprise when, on the basis of an approximate variational approach to the two-component Ginzburg-Landau model, Curty and Beck[4] recently predicted for certain parameter ranges the possibility of first-order phase transitions induced by phase fluctuations. In several papers[5–9] this quasianalytical[10] prediction was tested by Monte Carlo simulations and, as the main result, apparently confirmed numerically. If true, these findings would have an enormous impact on the theoretical description of many related systems such as superfluid helium, superconductors, certain liquid crystals, and possibly even the electroweak standard model of elementary particle physics.[11,12]

In view of these potential important implications for a broad variety of different fields we performed independent Monte Carlo simulations of the standard Ginzburg-Landau model in two and three dimensions in order to test whether the claim of phase-fluctuation-induced first-order transitions is a real effect or not.[13] Our results clearly support the prevailing opinion that the nature of the transition is of second order. In turn this implies, of course, that the variational approximation employed in Ref. 4 is less reliable than originally thought in view of the apparent numerical confirmations. In order to shed some light on the numerical results of Refs. 5–9, we generalized the standard model by adding a fugacity term which implicitly controls the vortex density of the model. The purpose of this paper is to present for this generalized Ginzburg-Landau model results on its phase structure as obtained from extensive Monte Carlo simulations. Employing finite-size scaling analyses we find numerical evidence that, by tuning the extra fugacity parameter, it is indeed possible to drive the system into a region with first-order phase transitions.

The layout of the remainder of this paper is organized as follows. In Sec. II we first recall the standard model and then discuss its generalization and the observables used to map out the phase diagram. Next we describe the employed simulation techniques in Sec. III. The results of our simulations are presented in Sec. IV, where we first discuss the three-dimensional case in some detail and then add a few brief comments on the two-dimensional model to complete the physical picture. Finally, in Sec. V we conclude with a summary of our main findings.

II. MODEL AND OBSERVABLES

The standard complex or two-component Ginzburg-Landau theory is defined by the Hamiltonian

$$H[\psi] = \int \mathrm{d}^d r \left[\alpha |\psi|^2 + \frac{b}{2} |\psi|^4 + \frac{\gamma}{2} |\nabla \psi|^2 \right], \quad \gamma > 0, \quad (1)$$

where $\psi(\vec{r}) = \psi_x(\vec{r}) + i\psi_y(\vec{r}) = |\psi(\vec{r})| e^{i\phi(\vec{r})}$ is a complex field and α, b, and γ are temperature-independent coefficients derived from a microscopic model. In order to carry out Monte Carlo simulations we put the model (1) on a d-dimensional hypercubic lattice with spacing a. Adopting the notation of Ref. 4, we introduce scaled variables $\tilde{\psi} = \psi / \sqrt{(|\alpha|/b)}$ and $\vec{u} = \vec{r}/\xi$, where $\xi = \sqrt{\gamma/|\alpha|}$ is the mean-field correlation length at zero temperature. This leads to the normalized lattice Hamiltonian

$$H[\tilde{\psi}] = k_B \tilde{V}_0 \sum_{n=1}^{N} \left[\frac{\tilde{\sigma}}{2} (|\tilde{\psi}_n|^2 - 1)^2 + \frac{1}{2} \sum_{\mu=1}^{d} |\tilde{\psi}_n - \tilde{\psi}_{n+\mu}|^2 \right], \quad (2)$$

with

$$\tilde{V}_0 = \frac{1}{k_B}\frac{|\alpha|}{b}\gamma a^{d-2}, \quad \tilde{\sigma} = \frac{a^2}{\xi^2}, \tag{3}$$

where μ denotes the unit vectors along the d coordinate axes, $N=L^d$ is the total number of sites, and an unimportant constant term has been removed. The parameter $\tilde{V}_0$ merely sets the temperature scale and can thus be absorbed in the definition of the reduced temperature $\tilde{T}=T/\tilde{V}_0$.

After these rescalings and omitting the tilde on ψ, σ, and T for notational simplicity in the rest of the paper, the partition function Z considered in the simulations is then given by

$$Z = \int D\psi D\overline{\psi} e^{-H/T}, \tag{4}$$

where

$$H[\psi] = \sum_{n=1}^{N}\left[\frac{\sigma}{2}(|\psi_n|^2-1)^2 + \frac{1}{2}\sum_{\mu=1}^{d}|\psi_n - \psi_{n+\mu}|^2\right] \tag{5}$$

and $\int D\psi D\overline{\psi} \equiv \int D\,\mathrm{Re}\psi D\,\mathrm{Im}\,\psi$ is short for integrating over all possible complex field configurations.

In Ref. 13 we have shown that the disagreement mentioned above is caused by an incorrect sampling of the Jacobian which emerges from the complex measure in Eq. (4) when transforming the field representation to polar coordinates, $\psi_n = R_n(\cos(\phi_n), \sin(\phi_n))$. When updating in the simulations the modulus $R_n=|\psi_n|$ and the angle ϕ_n, one has to rewrite the measure of the partition function (4) as

$$Z = \int_0^{2\pi} D\phi \int_0^{\infty} RDR e^{-H/T}, \tag{6}$$

where $DR \equiv \Pi_{n=1}^{N} dR_n$ and $R \equiv \Pi_{n=1}^{N} R_n$ is the Jacobian of this transformation. While mathematically indeed trivial (and of course properly taken into account in Ref. 4), this fact may easily be overlooked when coding the update proposals for the modulus and angle in a Monte Carlo simulation program. While for the angles it is correct to use update proposals of the form $\phi_n \to \phi_n + \delta\phi$ with $-\Delta\phi \leqslant \delta\phi \leqslant \Delta\phi$ (where $\Delta\phi$ is chosen such as to assure an optimal acceptance ratio), a similar procedure for the modulus, $R_n \to R_n + \delta R$ with $-\Delta R \leqslant \delta R \leqslant \Delta R$, would be incorrect since this ignores the R_n factor coming from the Jacobian. In fact, if we purposely ignore the Jacobian and simulate the model (6) (erroneously) without the R factor, then we obtain a completely different behavior than in the correct case; cf., e.g., Fig. 2 below. As already mentioned above these results reproduce[14] those in Refs. 5 and 9, and from this data one would indeed conclude evidence for a first-order phase transition when σ is small. With the correct measure, on the other hand, we have checked that *no* first-order signal shows up down to $\sigma=0.01$.

To treat the measure in Eq. (6) properly one can either use the identity $R_n dR_n = dR_n^2/2$ and update the squared moduli $R_n^2=|\psi_n|^2$ according to a uniform measure (where the update proposal $R_n^2 \to R_n^2 + \delta$ with $-\Delta \leqslant \delta \leqslant \Delta$ is correct) or one can introduce an effective Hamiltonian,

$$H_{\mathrm{eff}} = H - T\kappa\sum_{n=1}^{N}\ln R_n, \tag{7}$$

with $\kappa \equiv 1$, and work directly with a uniform measure for R_n. The incorrect omission of the R factor in Eq. (6) is equivalent to setting $\kappa=0$. It is well known[11] that the nodes $R_n=0$ correspond to core regions of vortices in the dual formulation of the model. The Jacobian factor R (or equivalently the term $-\Sigma \ln R_n$ in H_{eff}) tends to suppress field configurations with many nodes $R_n=0$. If the R factor is omitted, the number of nodes and hence vortices is relatively enhanced. It is thus at least qualitatively plausible that in this case a discontinuous, first-order "freezing transition" from a vortex dominated phase can occur, as is suggested by a similar mechanism for the XY model[11,15,16] and defect models of melting.[17,18]

In the limit of a large parameter σ, it is easy to read off from Eq. (5) that the modulus of the field is squeezed onto unity and once hence expects that irrespectively of the value of κ the XY model limit is approached with its well-known continuous phase transition in three dimensions (3D) at $T_c \approx 2.2$ and the Kosterlitz-Thouless (KT) transition in two dimensions (2D) at $T_{\mathrm{KT}} \approx 0.9$, respectively. While for the standard model with $\kappa=1$ this behavior should qualitatively persist for all values of σ, from the numerical results discussed above one expects that for $\kappa=0$ the order of the transition turns first order below a certain (tricritical) σ value. The purpose of this paper is to elucidate this behavior further by studying the phase diagram in the σ-κ plane—i.e., by considering an interpolating model with κ varying continuously between 0 and 1.

To be precise we always worked with the proper functional measure in Eq. (6) and replaced the standard Hamiltonian H by

$$H_{\mathrm{gen}} = H + T(1-\kappa)\sum_{n=1}^{N}\ln R_n = H + T\delta\sum_{n=1}^{N}\ln|\psi_n|, \tag{8}$$

where we have introduced the parameter $\delta=1-\kappa$, such that $\delta=0$ ($\kappa=1$) corresponds to the standard model and $\delta=1$ ($\kappa=0$) to the previously studied modified model with its first-order phase transition for small enough σ.

In order to map out the phase diagram in the σ-κ and σ-δ plane, respectively, we have measured in our simulations to be described in detail in the next section among other quantities the energy density $e=\langle H\rangle/N$, the specific heat per site $c_v=(\langle H^2\rangle - \langle H\rangle^2)/N$, and in particular the mean-square amplitude

$$\langle|\psi|^2\rangle = \frac{1}{N}\sum_{n=1}^{N}\langle|\psi_n|^2\rangle, \tag{9}$$

which will serve as the most relevant quantity for comparison with previous work.[4–9] For further comparison and in order to determine the critical temperature, the helicity modulus

$$\Gamma_\mu = \frac{1}{N}\left\langle \sum_{n=1}^{N} |\psi_n||\psi_{n+\mu}|\cos(\phi_n - \phi_{n+\mu}) \right\rangle - \frac{1}{NT}\left\langle \left[\sum_{n=1}^{N} |\psi_n||\psi_{n+\mu}|\sin(\phi_n - \phi_{n+\mu}) \right]^2 \right\rangle \quad (10)$$

was also computed. Notice that the helicity modulus Γ_μ is a direct measure of the phase correlations in the direction of μ. Because of cubic symmetry, all directions μ are equivalent and we always quote the average $\Gamma=(1/d)\Sigma_{\mu=1}^{d}\Gamma_\mu$. In the infinite-volume limit, Γ is zero above T_c and different from zero below T_c. We also have measured the vortex density v (of vortex points in 2D and vortex lines in 3D). The standard procedure to calculate the vorticity on each plaquette is by considering the quantity

$$m = \frac{1}{2\pi}([\phi_1 - \phi_2]_{2\pi} + [\phi_2 - \phi_3]_{2\pi} + [\phi_3 - \phi_4]_{2\pi} + [\phi_4 - \phi_1]_{2\pi}), \quad (11)$$

where $\phi_1, \ldots, \phi_4$ are the phases at the corners of a plaquette labeled, say, according to the right-hand rule and $[\alpha]_{2\pi}$ stands for α modulo 2π: $[\alpha]_{2\pi}=\alpha+2\pi n$, with n an integer such that $\alpha+2\pi n \in (-\pi,\pi]$, hence $m=n_{12}+n_{23}+n_{34}+n_{41}$. If $m\neq 0$, there exists a vortex which is assigned to the object dual to the given plaquette (a site in 2D and a link in 3D). Hence, in two dimensions, $*m$, the dual of m, is assigned to the center of the original plaquette. In three dimensions, the topological point charges are replaced by (oriented) line elements $*l_i$ which combine to form closed networks ("vortex loops"). The vortex "charges" $*m$ or $*l_i$ can take three values: $0, \pm 1$ (the values ± 2 have a negligible probability). The quantities

$$v = \frac{1}{L^2}\sum_x |*m_x| \quad (2\mathrm{D}), \quad (12)$$

$$v = \frac{1}{L^3}\sum_{x,i} |*l_{i,x}| \quad (3\mathrm{D}) \quad (13)$$

serve as a measure of the vortex density. We further analyzed the Binder cumulant

$$U = \frac{\langle(\vec{\mu}^2)^2\rangle}{\langle\vec{\mu}^2\rangle^2}, \quad (14)$$

where $\vec{\mu}=(\mu_x,\mu_y)$ with

$$\mu_x = \frac{1}{N}\sum_{n=1}^{N} \mathrm{Re}(\psi_n), \quad \mu_y = \frac{1}{N}\sum_{n=1}^{N} \mathrm{Im}(\psi_n), \quad (15)$$

is the magnetization per lattice site of a given configuration.

III. SIMULATION TECHNIQUES

Let us now turn to the description of the Monte Carlo update procedures used by us. To be on safe grounds, we started with the most straightforward (but most inefficient) algorithm known since the early days of Monte Carlo simulations: The standard Metropolis algorithm.[19] Here the complex field ψ_n is decomposed into its Cartesian components, $\psi_n=\psi_{x,n}+i\psi_{y,n}$. For each lattice site a random update proposal for the two components is made, e.g., $\psi_{x,n}\rightarrow\psi_{x,n}+\delta\psi_{x,n}$ with $\delta\psi_{x,n}\in[-\Delta,\Delta]$, and in the standard fashion accepted or rejected according to the energy change δH_{gen}. The parameter Δ is usually chosen such as to give an acceptance rate of about 50%, but other choices are permissible and may even result in a better performance of the algorithm (in terms of autocorrelation times). All this is standard[20] and guarantees in a straightforward manner that the complex measure $D\psi D\overline{\psi}$ in the partition function (4) is treated properly.

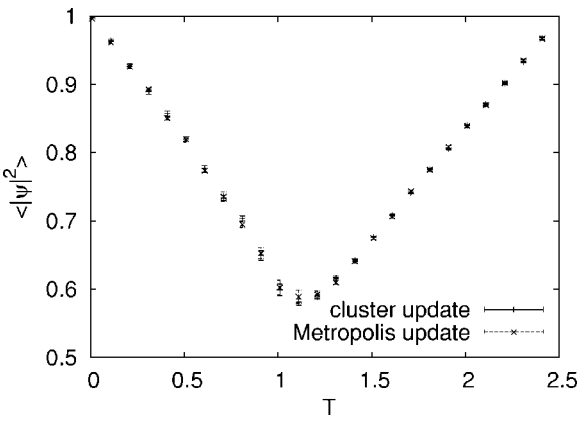

FIG. 1. Mean-square amplitude of the standard three-dimensional complex Ginzburg-Landau model with $\kappa=1$ and $\sigma=0.25$ on a 10^3 cubic lattice.

The well-known drawback of this algorithm is its critical slowing down (large autocorrelation times) in the vicinity of a continuous phase transition,[20] leading to large statistical errors for a fixed computer budget. To improve the accuracy of our data we therefore employed the single-cluster algorithm[21] to update the direction of the field,[22] similar to simulations of the XY spin model.[23] The modulus of ψ is updated again with a Metropolis algorithm. Here some care is necessary to treat the measure in Eq. (4) properly (see above comments). Per measurement we performed one sweep with the Metropolis algorithm and n single-cluster updates. For all simulations in two and three dimensions the number of cluster updates was chosen such that $n\langle|C|\rangle\approx L^d\equiv N$, where $\langle|C|\rangle$ is the average cluster size. Since $\langle|C|\rangle$ scales with system size as the susceptibility, $\chi=N\langle\vec{\mu}^2\rangle\simeq L^{\gamma/\nu}$, and $\gamma/\nu=2-\eta=7/4$ at the Kosterlitz-Thouless transition in 2D and $\gamma/\nu=2-\eta\approx 2$ in 3D, n was chosen $\propto L^{1/4}$ in 2D and $\propto L$ in 3D. In the 2D case most of the simulations were performed for $L=10$, 20, and 40, and in 3D we usually studied the lattice sizes $L=10$, 15, 20, and 30. For each simulation point we thermalized with 500–1000 sweeps and averaged the measurements over 10 000 sweeps. In the cases of strong first-order phase transitions we employed a variant of the multicanonical scheme[24] where the histogram of the mean modulus is flattened instead that of the energy. All error bars are computed with the Jackknife method.[25] In the following we only show the more extensive and accurate data set of the cluster simulations, but we tested in many

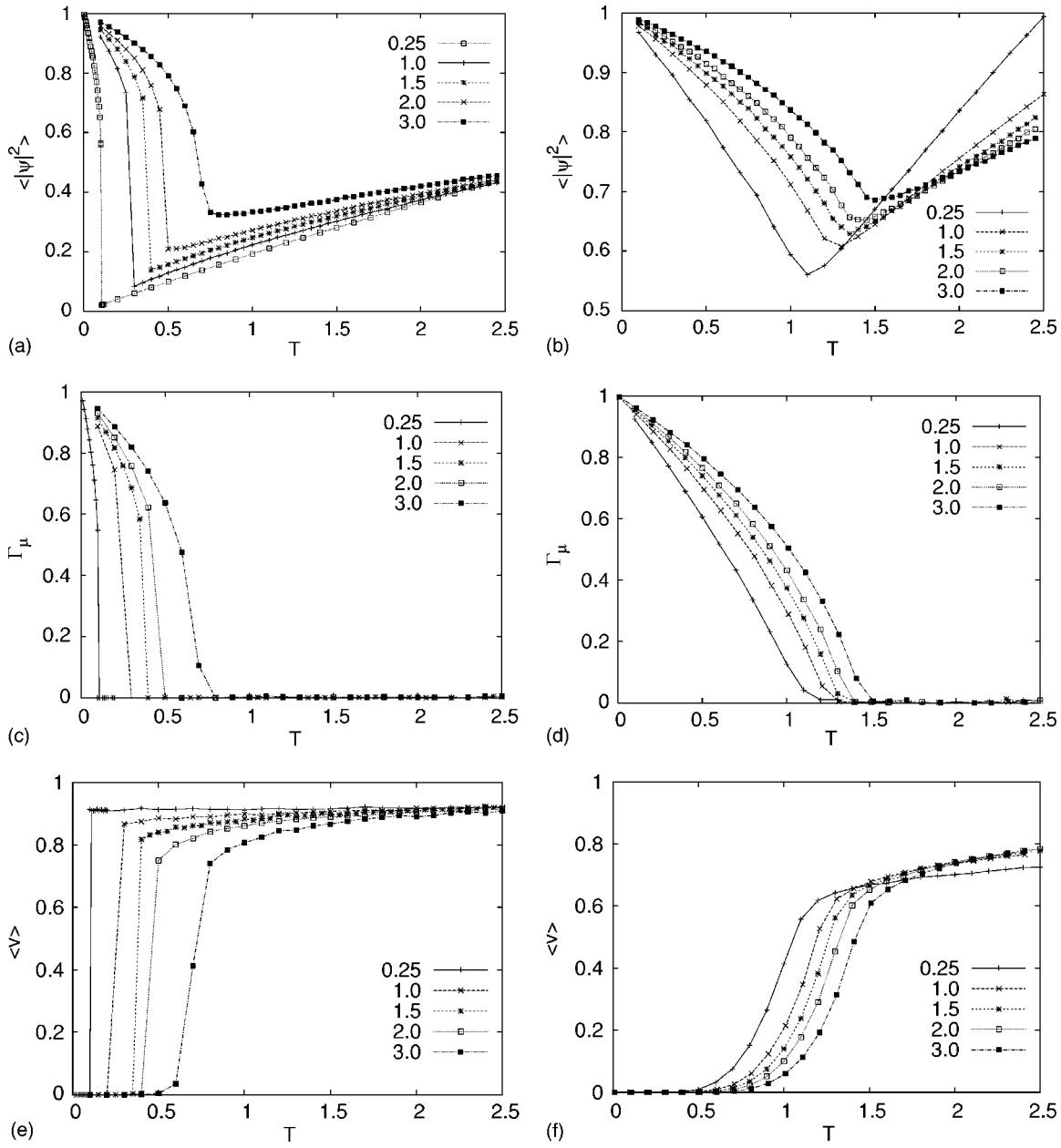

FIG. 2. Mean-square amplitude $\langle|\psi|^2\rangle$, helicity modulus Γ_μ, and vortex-line density $\langle v\rangle$ of the three-dimensional generalized complex Ginzburg-Landau model on a 15^3 cubic lattice for different values of the parameter $\sigma=0.25,\ldots,3.0$ for the case $\kappa=0$ (left) and the standard formulation with $\kappa=1$ (right).

representative cases that the Metropolis simulations coincide within error bars; for an example, see Fig. 1.

IV. RESULTS

A. Three dimensions

In the first set of simulations we concentrated on the two most characteristic cases $\kappa=0$ and $\kappa=1$ and performed temperature scans on a 15^3 lattice for various values of the parameter σ. Our results for the mean-square amplitude, the helicity modulus, and the vortex-line density are compared for the two cases in Fig. 2. In the plots for $\kappa=0$ on the left side, we see that all three quantities exhibit quite pronounced jumps for small σ values, which is a clear indication that in this regime the phase transition is of first order. At $\sigma=0.25$, for example, we observe already on very small lattices a clear double-peak structure for the distributions of the energy and mean-square amplitude as well as the mean modulus $|\psi|=(1/N)\Sigma_{n=1}^{N}|\psi_n|$ which is depicted in Fig. 3. Notice that already for the extremely small lattice size of 4^3 the minimum between the two peaks is suppressed by more than 20 orders of magnitude. This is an unambiguous indication for two coexisting phases and thus clearly implies that the model undergoes a first-order phase transition in the small-σ regime for $\kappa=0$. Due to the pronounced metastability, these simulations had to be performed with a variant of the multicanoni-

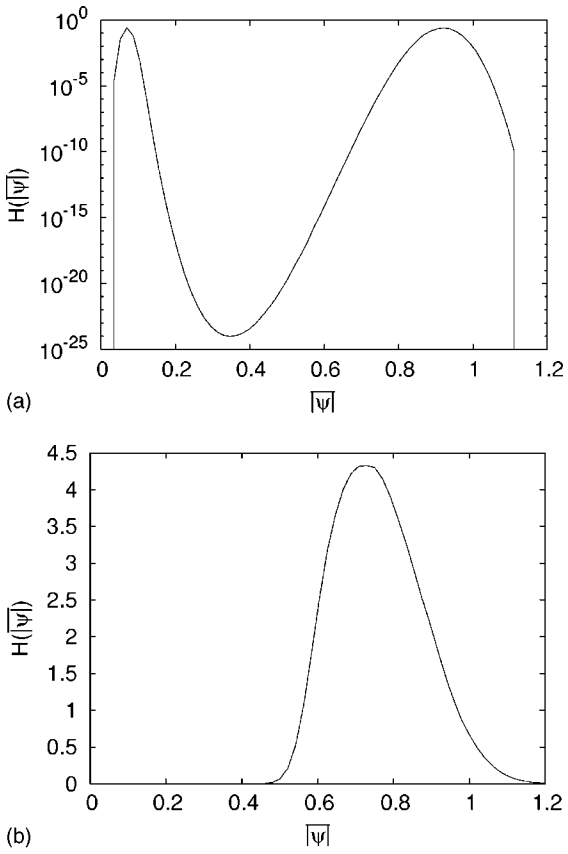

FIG. 3. Top: histogram of the mean modulus $\overline{|\psi|}$ on a logarithmic scale for a 4^3 cubic lattice, $\kappa=0$ and $\sigma=0.25$, reweighted to the temperature $T_0\approx 0.0572$ where the two peaks are of equal height. Bottom: histogram for the same quantity and lattice size at $T=1.1$ close to the second-order phase transition for $\kappa=1$ and $\sigma=0.25$.

cal scheme[24] where, instead of flattening the energy histogram, extra weight factors for the mean modulus were introduced. With this simulation technique we overcome the difficulty of sampling the extremely rare events between the two peaks of the canonical distribution. A closer look at the $\kappa=0$ plots shows that the crossover from second- to first-order transitions happens around $\sigma_t\approx 2.5$. For the standard model with $\kappa=1$, on the other hand, we observe for *all* σ values a smooth behavior, suggesting that the *XY*-model-like continuous transition persists also for small σ values. This is clearly supported by a single-peak structure of all distributions just mentioned; for the case of the mean modulus, see Fig. 3. This supports the prevailing opinion that the standard complex $|\psi|^4$ model always undergoes a second-order phase transition. In fact, we have checked that down to $\sigma=0.01$ *no* signal of a first-order transition can be detected for the standard model parametrized by $\kappa=1$. The resulting transition lines in the σ-T plane for $\kappa=0$ and $\kappa=1$ are sketched in Fig. 4, with the thick line for $\kappa=0$ indicating the approximate regime of first-order phase transitions.

Next we concentrated on the small σ regime and performed a rough finite-size scaling (FSS) analysis for $\sigma=0.25$ on moderately large 10^3, 15^3, 20^3, and 30^3 lattices. In Fig. 5 we compare results for the energy, mean-square amplitude (9), helicity modulus (10), and vortex-line density

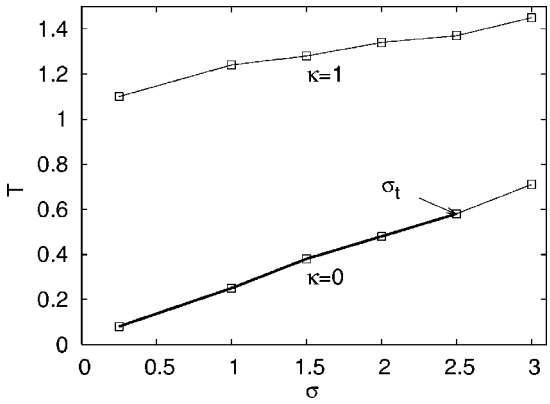

FIG. 4. Transition lines in the σ-T plane for $\kappa=0$ and $\kappa=1$. The thick line for $\kappa=0$ indicates first-order phase transitions while all other transitions are continuous.

(13) for $\kappa=0$ and $\kappa=1$. Apart from the transition region where a strong size dependence is of course expected, we notice only a small dependence on the variation of the lattice size. On the basis of these results, we do not expect a significant change of the qualitative behavior for much larger lattices and hence used similar moderate lattice sizes for most of our further investigations.

To exemplify the big differences between the models with $\kappa=0$ and $\kappa=1$, we choose in the following the case $\sigma=1.5$, where we shall characterize for both κ values the phase transitions in some detail. Let us start with the nonstandard case $\kappa=0$, where the first-order phase transition around $T\approx 0.36$ is also pronounced but much less strong than for $\sigma=0.25$. Still, in order to get sufficiently accurate equilibrium results, the simulations for lattices of size $L=4$, 6, 8, 10, 12, 14, 15, and 16 had to be performed again with our modulus variant of the multicanonical method. As can be inspected in the histogram plots for the mean modulus shown in Fig. 6, the frequency of the rare events between the two peaks in the canonical ensemble for a 16^3 lattice is about 50 orders of magnitude smaller than for configurations contributing to the two peaks.

In order to characterize the transition more quantitatively we estimated the interface tension[26]

$$F_L^s = \frac{1}{2L^{d-1}} \ln \frac{P_L^{\max}}{P_L^{\min}}, \tag{16}$$

where $P_L^{\max}$ is the value of the two peaks and $P_L^{\min}$ denotes the minimum in between. Here we have assumed that for each lattice size the temperature was chosen such that the two peaks are of equal height which can be achieved by histogram reweighting. The thus defined temperatures approach the infinite-volume transition temperature as $1/L^d$, and for the final estimate of $F^s=\lim_{L\to\infty} F_L^s$, we performed a fit according to[27]

$$F_L^s = F^s + \frac{a}{L^{d-1}} + \frac{b\ln(L)}{L^{d-1}}. \tag{17}$$

As is shown in Fig. 6, the finite-lattice estimates F_L^s are clearly nonzero. The infinite-volume extrapolation (17) tends

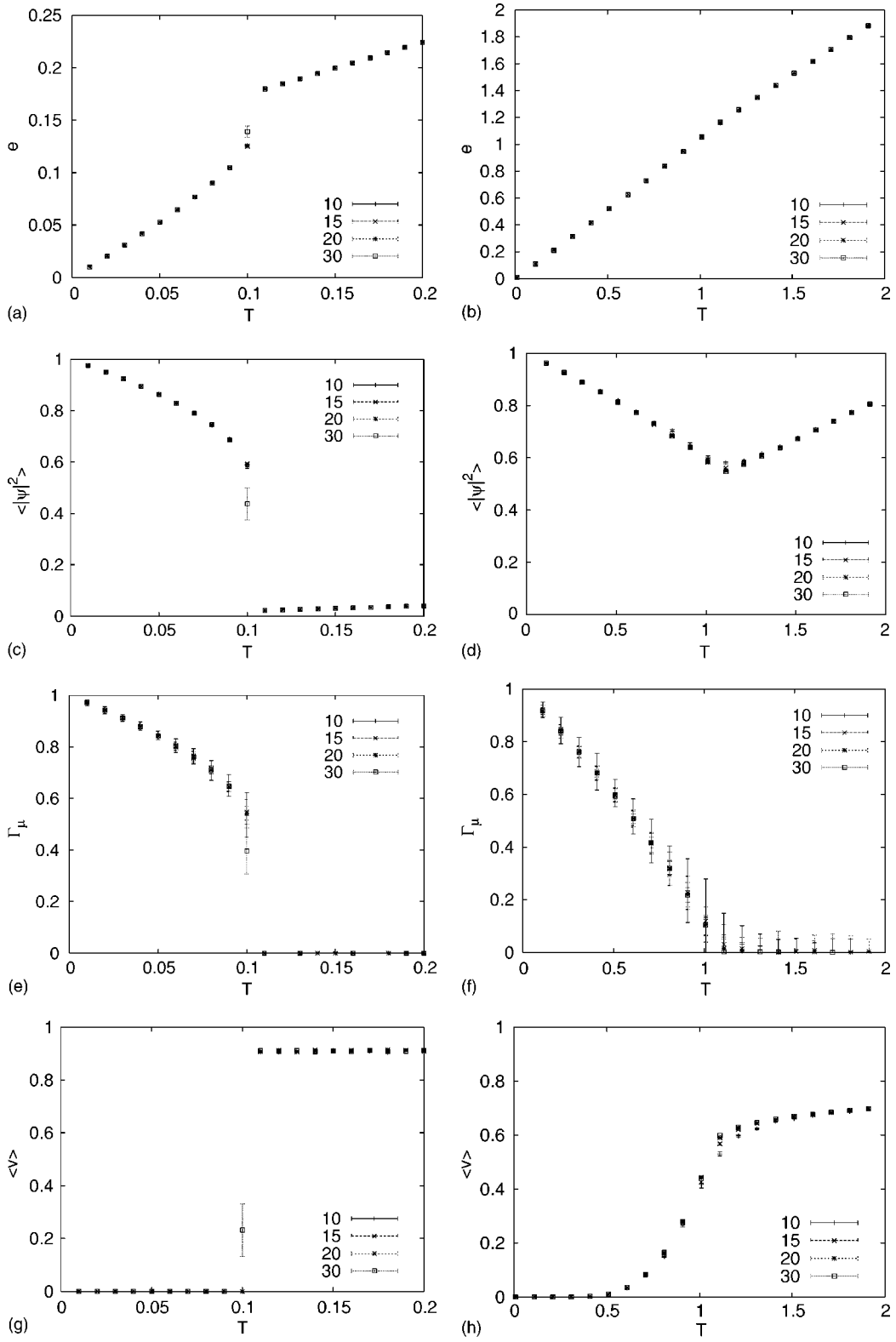

FIG. 5. Energy density e, mean-square amplitude $\langle|\psi|^2\rangle$, helicity modulus Γ_μ, and vortex-line density $\langle v\rangle$ on 10^3, 15^3, 20^3, and 30^3 cubic lattices for $\sigma=0.25$ and $\kappa=0$ (left) and $\kappa=1$ (right), respectively.

to increase with system size and yields a comparably large interface tension of $F^s=0.271(5)$.

Let us now turn to the second generic case $\kappa=1$, where the model definitely exhibits for $\sigma=1.5$ a second-order phase transition around $\beta\equiv 1/T\approx 0.8$. To confirm the expected critical exponents of the $O(2)$ or XY model universality class, we simulated here close to criticality somewhat larger lattices of size $L=4$, 8, 12, 16, 20, 24, 32, 40, and 48 and

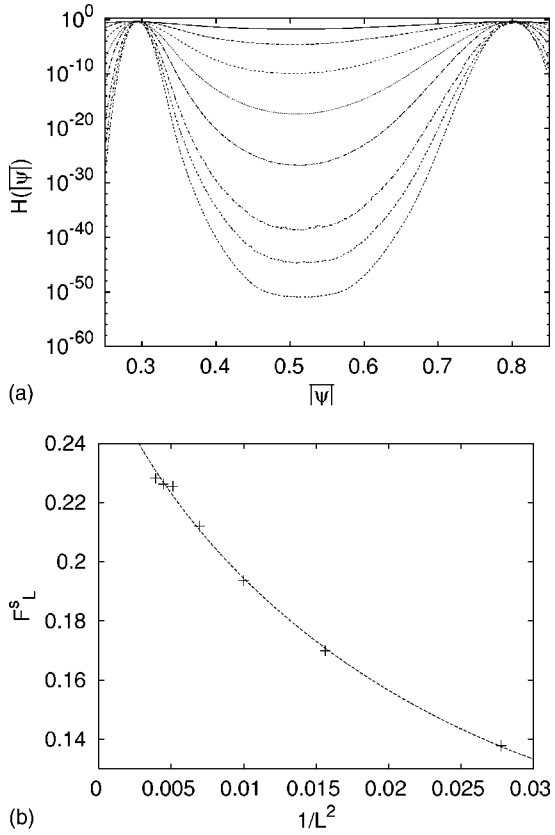

FIG. 6. Top: histogram of the mean modulus $\overline{|\psi|}$ for $\kappa=0$ and $\sigma=1.5$ on a logarithmic scale for various lattice sizes ranging from $L=4$ (top curve) to $L=16$ (bottom curve), reweighted to temperatures where the two peaks are of equal height. Bottom: FSS extrapolation for $L\geqslant 6$ of the interface tension F_L^s, yielding the infinite-volume limit $F^s=0.271(5)$.

performed a standard FSS analysis. From short runs we first estimated the location of the phase transition to be at $\beta_0=0.7795\approx\beta_c$. In the long runs at β_0 we recorded the time series of the energy density $e=E/N$, the magnetization $\vec{\mu}$, the mean modulus $\overline{|\psi|}$, and the mean-square amplitude[28] $|\psi|^2$, as well as the helicity modulus Γ_μ and the vorticity v. After an

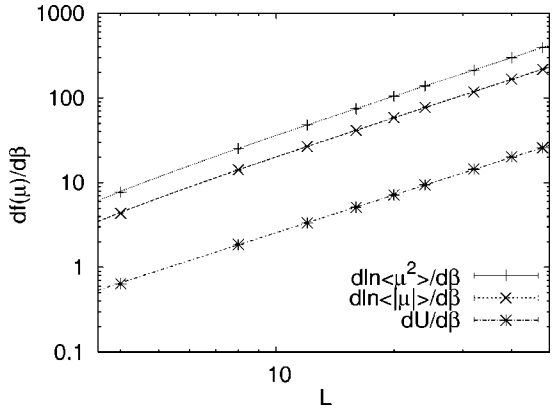

FIG. 7. Least-squares fits for $\kappa=1$ and $\sigma=1.5$ on a log-log scale, using the FSS ansatz $df(\mu)/d\beta\propto L^{1/\nu}$ at the maxima locations. The fits using the data for $L\geqslant 8$ lead to an overall critical exponent $1/\nu=1.493(7)$ or $\nu=0.670(3)$.

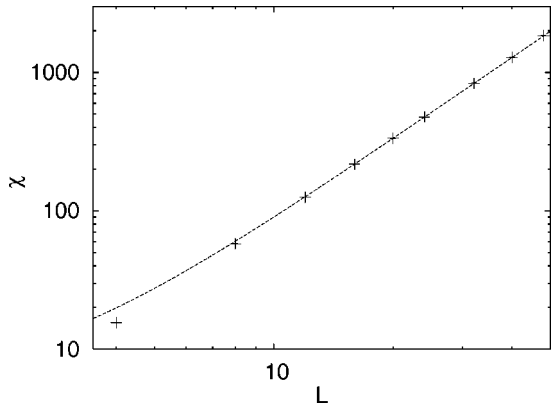

FIG. 8. Log-log plot of the FSS of the susceptibility for $\kappa=1$ and $\sigma=1.5$ at $\beta=0.780\,08\approx\beta_c$. The line shows the three-parameter fit $a+bL^{\gamma/\nu}$, yielding for $L\geqslant 16$ the estimate $\gamma/\nu=1.962(12)$.

initial equilibration time we took about 1 000 000 measurements for each lattice size. Applying the reweighting technique we first determined the maxima of the susceptibility, $\chi'=N(\langle\vec{\mu}^2\rangle-\langle|\vec{\mu}|\rangle^2)$, of $d\langle|\vec{\mu}|\rangle/d\beta$, and of the logarithmic derivatives $d\ln\langle|\vec{\mu}|\rangle/d\beta$ and $d\ln\langle\vec{\mu}^2\rangle/d\beta$. The locations of these maxima provide us with four sequences of pseudo-transition points $\beta_{\max}(L)$ for which the scaling variable $x=(\beta_{\max}(L)-\beta_c)L^{1/\nu}$ should be constant. Using this fact we then have several possibilities to extract the critical exponent ν from (linear) least-squares fits of the FSS ansatz $dU_L/d\beta\cong L^{1/\nu}f_0(x)$ or $d\ln\langle|\vec{\mu}|^p\rangle/d\beta\cong L^{1/\nu}f_p(x)$ to the data at the various $\beta_{\max}(L)$ sequences. The quality of our data and the fits starting at $L_{\min}=8$, with goodness-of-fit parameters $Q=0.85-0.90$, can be inspected in Fig. 7. All resulting exponent estimates and consequently also their weighted average,

$$1/\nu=1.493(7),\quad \nu=0.670(3), \tag{18}$$

are in perfect agreement with recent high-precision Monte Carlo estimates for the XY model universality class.[22,29] Note that hyperscaling implies $\alpha=2-3\nu=-0.010(9)$, which also favorably compares with recent spacelab experiments on the λ transition in liquid helium.[30]

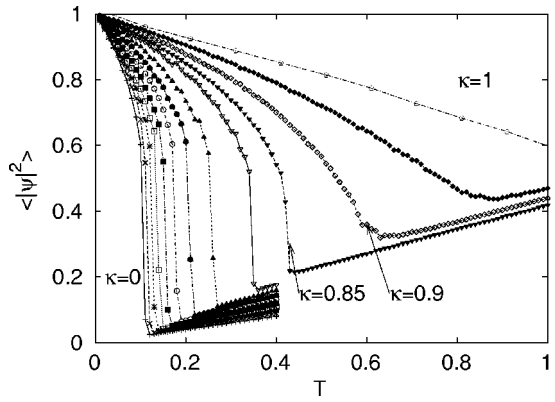

FIG. 9. The κ dependence of the mean-square amplitude $\langle|\psi|^2\rangle$ as a function of temperature on a 15^3 lattice for $\sigma=0.25$.

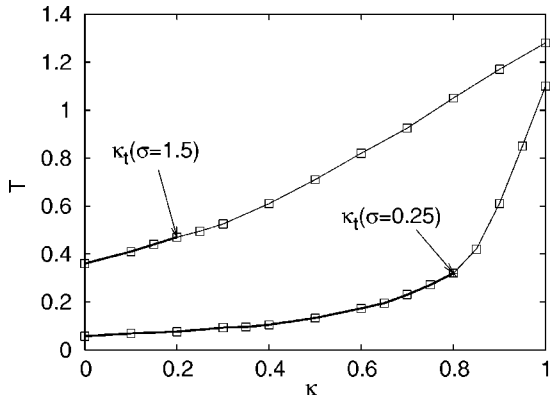

FIG. 10. Phase diagram in the κ-T plane of the three-dimensional generalized complex Ginzburg-Landau model for $\sigma=0.25$ and $\sigma=1.5$. The transitions along the thick line for $\kappa<\kappa_t$ are of first order, and the transitions for $\kappa>\kappa_t$ are of second order. The points labeled κ_t at the intersection of these two regimes are tricritical points.

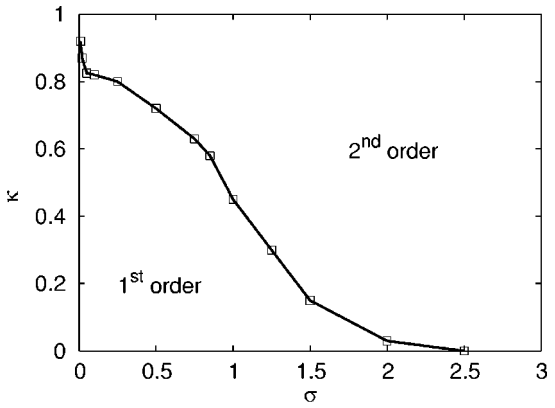

FIG. 11. Phase structure in the σ-κ plane of the generalized complex Ginzburg-Landau model in three dimensions, separating regions with first- and second-order phase transitions, respectively, when the temperature is varied. All continuous transitions fall into the universality class of the XY model which is approached for all κ-values in the limit $\sigma\to\infty$.

Assuming thus $1/\nu=1.493$ we can improve our estimate for β_c from linear least-squares fits to the scaling behavior of the various $\beta_{\max}$ sequences. The combined estimate from the four sequences is $\beta_c=0.780\,08(4)$. To extract the critical exponent ratio γ/ν we can now use the scaling relation for the susceptibility $\chi=N\langle\vec{\mu}^2\rangle\simeq a+bL^{\gamma/\nu}$ at β_c. For $L\geqslant 16$ we obtain from the FSS fit with $Q=0.70$ shown in Fig. 8 the estimate of

$$\gamma/\nu=1.962(12)[9], \tag{19}$$

where we also take into account the uncertainty in our estimate of β_c; this error is estimated by repeating the fit at $\beta_c\pm\Delta\beta_c$ and indicated by the number in square brackets. Here we find a slight dependence of this value on the lower bound of the fit range $[L_{\min},48]$; i.e., one would have to include larger lattices for a high-precision estimate of the critical exponent ratio γ/ν, but this was not our objective here. Still, these results are in good agreement with recent high-precision estimates in the literature[22,29] and clearly confirm the expected second-order nature of the phase transition in the standard complex $|\psi|^4$ model, governed by XY model critical exponents.

A similar set of simulations for $\sigma=0.25$ at $\beta_c=0.9284(4)$ for lattice sizes $L=4$, 8, 12, 14, 16, 20, 24, 28, 32, and 40 gave the exponent estimates $1/\nu=1.498(9)$, $\nu=0.668(4)$, and $\gamma/\nu=1.918(71)[8]$, which are less accurate but again compatible with the XY model universality class. At any rate these results definitely rule out the possibility of a first-order phase transition in the standard model at small σ values. When going to even smaller σ values, the FSS analysis is more and more severely hampered by the vicinity of the Gaussian fixed point which induces strong crossover scaling effects. Since consequently very large system sizes would be required to see the true, asymptotic (XY-model-like) critical behavior we have not further pursued our attempts in this direction. Here we only add the remark that for $\sigma=0.01$ the energy and magnetization distributions exhibit a clear single-peak structure for all considered lattice sizes up to $L=20$, showing that in the standard model with $\kappa=1$ a phase-fluctuation induced first-order phase transition is very unlikely even for very small σ values.

We also checked the critical behavior along the line of second-order transitions for $\kappa=0$. Specifically, at $\sigma=5$—i.e., sufficiently far away from the crossover to first-order transitions at $\sigma_t\approx 2.5$—we obtained from FSS fits to data at $\beta_c=0.97253(4)$ for lattices of size $L=4$, 8, 12, 16, 20, 24, 28, 32, and 40 the exponent estimates $1/\nu=1.489(7)$, $\nu=0.671(3)$, and $\gamma/\nu=1.913(82)[13]$. As expected by symmetry arguments, also these results for the second-order regime of the $\kappa=0$ variant of the model are in accord with the XY model universality class.

In a second set of simulations we explored the two-dimensional σ-κ parameter space of the generalized Ginzburg-Landau model in the orthogonal direction by performing simulations at fixed σ values and κ varying from $\kappa=0$ to 1. For the most σ values we concentrated on the crossover region between first- and second-order phase transitions when varying κ. For two selected values $\sigma=0.25$ and $\sigma=1.5$, we studied the κ dependence more systematically by simulating all values from $\kappa=0$ to 1 in steps of 0.1. In addition we performed two further runs in the crossover regime at $\kappa=0.85$ and 0.95 for $\sigma=0.25$ as well as at $\kappa=0.15$ and $\kappa=0.25$ for $\sigma=1.5$. In Fig. 9 we show the resulting mean-square amplitudes for all simulated values of κ at $\sigma=0.25$ as a function of the temperature, indicating again that for small κ the transitions are first-order like while for κ closer to unity the expected second-order transitions emerge. From Fig. 9 we read off that for $\sigma=0.25$ the crossover between the two types of phase transitions happens around $\kappa_t(\sigma=0.25)\approx 0.8$, and the analogous analysis for $\sigma=1.5$ yields $\kappa_t(\sigma=1.5)\approx 0.2$. The resulting transition lines for these two σ values are plotted in Fig. 10, where the thick lines indicate again first-order phase transitions.

Finally, by combining all numerical evidences collected so far with additional data not described here in detail, we find the phase structure in the σ-κ plane depicted in Fig. 11. All points in the lower left corner for small σ and small κ

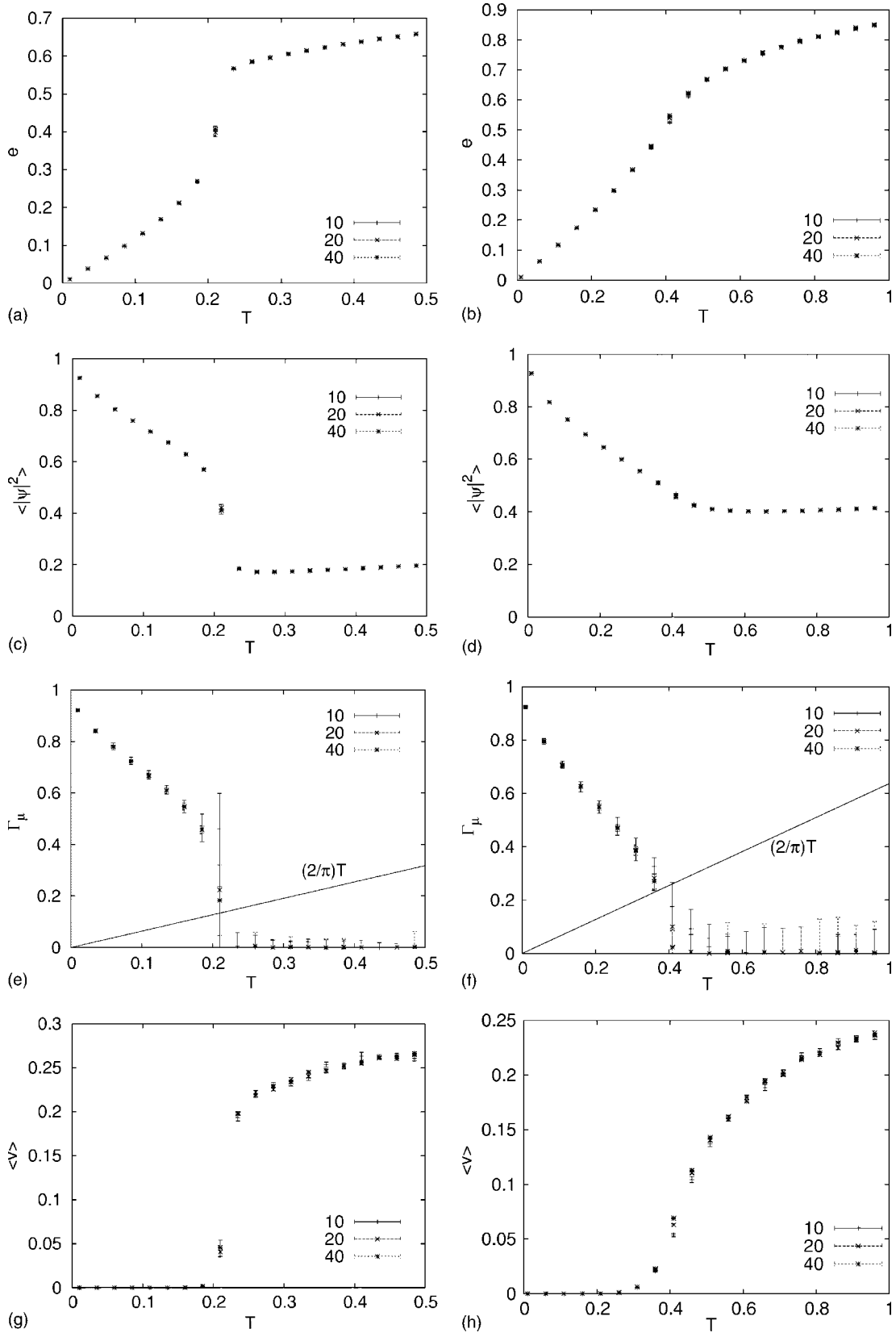

FIG. 12. Energy density e, mean-square amplitude $\langle|\psi|^2\rangle$, helicity modulus Γ_μ, and vortex density $\langle v\rangle$ of the two-dimensional model on 10^2, 20^2, and 40^2 square lattices for $\sigma=1$ and $\kappa=0$ (left) and $\kappa=1$ (right), respectively. The straight line in the Γ_μ plots indicates the universal KT jump $\Gamma_\mu=(2/\pi)T$ at $T=T_c$, which clearly is only compatible with the data for the standard model with $\kappa=1$.

exhibit temperature-driven first-order phase transition when the temperature is varied, while all points in the upper right corner display a continuous transition of the *XY* model type. This means in particular that for the standard model parameterized by $\kappa=1$ this is always true. Quantitatively the *XY* model is reached for all κ values in the limiting case $\sigma \to \infty$.

B. Two dimensions

We conclude the paper with a few very brief remarks on the two-dimensional generalized model where the Kosterlitz-Thouless nature of the standard *XY* model transition would require more care for a precise study. Here we only report results of some runs at $\sigma=1$ for 10^2, 20^2, and 40^2 square lattices. As the main result, we find that the standard observables e, $\langle|\psi|^2\rangle$, Γ, and $\langle v\rangle$ exhibit qualitatively the same pattern as in three dimensions. This is demonstrated in Fig. 12 where again the two cases $\kappa=0$ and $\kappa=1$ are compared. For $\kappa=0$, the data are indicative of a first-order transition around $T\approx 0.2$, while the behavior of the standard model with $\kappa=1$ is consistent with the expected Kosterlitz-Thouless transition around $T\approx 0.4$. Note in particular that (only) the data for $\kappa=1$ are compatible with the expected universal jump of the helicity modulus at T_c, $\Gamma_\nu=(2/\pi)T$, indicated by the straight line in the corresponding plots. A careful investigation of the first-order transitions in the generalized model with $\kappa=0$ will be reported elsewhere.

V. SUMMARY

The possibility of a phase-fluctuation-induced first-order phase transition in the standard three-dimensional Ginzburg-Landau model as suggested by approximate variational calculations[4] cannot be confirmed by our numerical simulations down to very small values of the parameter σ. Our results suggest, however, that a generalized Ginzburg-Landau model can be tuned to undergo first-order transitions by a mechanism similar to that discussed in Ref. 15 when varying the parameter κ of an additional $\Sigma \ln R_n$ term in the generalized Hamiltonian (8). As in Ref. 15 this can be understood by a duality argument. For $0 \leqslant \kappa < 1$ the extra term reduces the ratio of core energies of vortex lines of vorticity two versus those of vorticity one, and this leads to the same type of transition as observed in defect melting of crystals.

The phase transitions of the standard model as well as the continuous transitions of the generalized model are confirmed to be governed by the critical exponents of the *XY* model or $O(2)$ universality class, as expected by general symmetry arguments. For the generalized model it would be interesting to analyze in more detail the tricritical points separating the regions with first- and second-order phase transitions. Such a study, however, is quite a challenging project and hence left for the future.

Exploratory simulations of the two-dimensional case, where the standard model exhibits Kosterlitz-Thouless transitions, indicate that a similar mechanism can drive the transition of the generalized model to first order also there.

ACKNOWLEDGMENTS

E.B. thanks the EU network HPRN-CT-1999-00161 EUROGRID, "Geometry and Disorder: from membranes to quantum gravity," for a grant. Partial support by the German-Israel-Foundation (GIF) under Contract No. I-653-181.14/1999 is also gratefully acknowledged.

[1] J. Zinn-Justin, *Quantum Field Theory and Critical Phenomena*, 3rd ed. (Clarendon Press, Oxford, 1996).
[2] H. Kleinert and V. Schulte-Frohlinde, *Critical Properties of* Φ^4*-Theories* (World Scientific, Singapore, 2001).
[3] H. Kleinert, Phys. Rev. Lett. **84**, 286 (2000).
[4] P. Curty and H. Beck, Phys. Rev. Lett. **85**, 796 (2000).
[5] P. Curty and H. Beck, cond-mat/0010084 (unpublished).
[6] H. Fort, hep-th/0010070 (unpublished).
[7] G. Alvarez and H. Fort, Phys. Rev. B **63**, 132504 (2001).
[8] G. Alvarez and H. Fort, Phys. Lett. A **282**, 399 (2001).
[9] G. Alvarez and H. Fort, Phys. Rev. B **64**, 092506 (2001).
[10] The method of Ref. 4 uses *XY* model data as input.
[11] H. Kleinert, *Gauge Fields in Condensed Matter* (World Scientific, Singapore, 1989), Vol. I.
[12] V. M. Loktev, R. M. Quick, and S. G. Sharapov, Phys. Rep. **349**, 1 (2001).
[13] E. Bittner and W. Janke, Phys. Rev. Lett. **89**, 130201 (2002).
[14] There is another difference between our update and the update described in the Refs. 5 and 9: namely, that we do *not* restrict the modulus of the field to a finite interval. This can cause further systematic deviations but we explicitly checked that this is unimportant for the main point here.
[15] W. Janke and H. Kleinert, Nucl. Phys. B **270**, 399 (1986).
[16] P. Minnhagen and M. Wallin, Phys. Rev. B **36**, 5620 (1987); G.-M. Zhang, H. Chen, and X. Wu, *ibid.* **48**, 12 304 (1993); D. Yu. Irz, V. N. Ryzhov, and E. E. Tareyeva, *ibid.* **54**, 3051 (1996).
[17] H. Kleinert, *Gauge Fields in Condensed Matter* (World Scientific, Singapore, 1989), Vol. II.
[18] W. Janke, Int. J. Theor. Phys. **29**, 1251 (1990).
[19] N. Metropolis, A. W. Rosenbluth, M. N. Rosenbluth, A. H. Teller, and E. Teller, J. Chem. Phys. **21**, 1087 (1953).
[20] W. Janke, Math. Comput. Simul. **47**, 329 (1998); in *Computational Physics: Selected Methods—Simple Exercises—Serious Applications*, edited by K. H. Hoffmann and M. Schreiber (Springer, Berlin, 1996), pp. 10–43.
[21] U. Wolff, Phys. Rev. Lett. **62**, 361 (1989); Nucl. Phys. B **322**, 759 (1989).
[22] M. Hasenbusch and T. Török, J. Phys. A **32**, 6361 (1999).
[23] W. Janke, Phys. Lett. A **148**, 306 (1990).
[24] B. A. Berg and T. Neuhaus, Phys. Lett. B **267**, 249 (1991); Phys. Rev. Lett. **68**, 9 (1992).
[25] B. Efron, *The Jackknife, the Bootstrap and Other Resampling Plans* (Society for Industrial and Applied Mathematics [SIAM], Philadelphia, 1982).
[26] W. Janke, in *Computer Simulations of Surfaces and Interfaces*,

NATO Science Series II, Mathematics, Physics and Chemistry, Vol. 114, Proceedings of the NATO Advanced Study Institute, Albena, Bulgaria, 2002, edited by B. Dünweg, D. P. Landau, and A. I. Milchev (Kluwer, Dordrecht, 2003), pp. 111–135.

[27] U. Hansmann, B. A. Berg, and T. Neuhaus, Int. J. Mod. Phys. C **3**, 1155 (1992).

[28] Recall that $\overline{|\psi|} \equiv \Sigma_{n=1}^{N} |\psi_n| / N$ and $|\psi|^2 \equiv \Sigma_{n=1}^{N} |\psi_n|^2 / N$, such that $\overline{|\psi|}^2 \neq |\psi|^2$.

[29] M. Campostrini, M. Hasenbusch, A. Pelissetto, P. Rossi, and E. Vicari, Phys. Rev. B **63**, 214503 (2001).

[30] J. A. Lipa, J. A. Nissen, D. A. Stricker, D. R. Swanson, and T. C. P. Chui, Phys. Rev. B **68**, 174518 (2003).